Draft version December 14, 2022
Typeset using LaTeX **twocolumn** style in AASTeX631

GRMHD Simulations are not Agnostic to Initial Conditions

Vikram Manikantan [1]

[1] *Department of Astronomy, University of Arizona, Tucson, AZ, USA*

ABSTRACT

For the past decade, we have seen the immense progress of large-scale simulations of high-energy, compact object systems. Often, a general-relativistic magnetohydrodynamic (GRMHD) code is used to evolve an accretion disk around a compact object (black hole or neutron star). However, the initial conditions of this accretion disk are a choice, rather than scientifically backed. This is because accretion disk formation methods are still being understood, and simulating the full timescale of formation to steady-state is currently beyond the capabilities of most computing allocations. More specifically, we do not know how our chosen initial conditions impact the final result of a simulation. To remedy this, we study three popular accretion disk initial conditions and simulate them out to $10,000\ r_g/c$. In our resolution-limited simulations, we find that initial conditions do have an affect on the final mass accretion rate of the system. However, numerous variables across the different simulations are not kept consistent. Therefore we cannot conclude whether it is the structure of the solutions or arbitrary differences in simulation set-up that cause these differences. Further studies of these simulations in higher resolution and longer evolution times will provide further insight into the true impact of initial conditions on GRMHD simulations.

Keywords: Black Holes (162) — Accretion (14) — Magnetohydrodynamical Simulations (1966)

1. INTRODUCTION

Black holes (BHs) are responsible for some of the most energetic and luminous outflows in the universe. There is a diverse selection of BH-powered phenomena including, but not limited to, long gamma-ray bursts, tidal disruptions events, and state transitions in X-ray binaries. While the source of the gas supply that accretes onto the BH varies in each of these scenarios, they all form accretion disks and their luminous end results depend sensitively on the characteristics of the accretion disk. These characteristics include, amongst many others: magnetization (β), density (ρ), disk thickness ($\frac{H}{R}$), and mass accretion rate ($\dot{M}$).

To understand how these different variables affect the BH-Accretion Disk system, we have relied on large-scale general relativistic magnetohydrodynamic simulations (GRMHD). These codes, such as Athena++ (Stone et al.) and H-AMR (Liska et al.), simulate the evolution of an accretion disk around compact objects on a curved spacetime according to magnetohydrodynamic fluid equations (Gammie et al. 2003). The physics of the evolution of an accretion disk is quite well understood - recent developments have included radiation transport, two temperature schemes and numerical relativity, leading to a suite of simulations that provide even more insight into physical processes in the accretion disk, such as current sheets and disk cooling. However, the initial conditions for the accretion disk are still a matter of choice. Furthermore, previous studies have shown that the Bernoulli parameter, a measure of how bound to the central object material in the system is, is dependent on the initial conditions (Penna et al. 2013). In other words, the evolution of the accretion disk is dependent on its initial conditions.

Penna et al. (2013) investigates this very issue by studying the behavior of the bernoulli parameter with time. They take two previous simulations and show that the final profile of the bernoulli parameter is tightly linked to the initial conditions, prompting them to develop a modified solution of Chakrabarti (1985). However, they do not then show that this new solution is agnostic to initial conditions over time.

Corresponding author: Vikram Manikantan
vik@arizona.edu

The goal of this study is to, for the first time, compare three solutions for the initial conditions of a magnetized torus around a compact object to determine the effect of initial conditions on the final evolution of the accretion disk, using the bernoulli parameter. The two most popular solutions in the field are the Fishbone & Moncrief (1976) torus (FM torus) and the Chakrabarti (1985) torus, also known as the power-law solution (PL torus). Lastly, I will also include Penna et al.'s modified power-law torus solutions (Modified PL). Furthermore, by expanding my metric of measurements to magnetization and density profiles, I will be able to determine the possible use cases for each of the initial conditions set forth.

In section 2, I describe the initial set up for the simulations performed and analyzed in this paper, in section 3 I present the mathematical solutions to the intial conditions of the torii I simulate (Fishbone & Moncrief 1976; Chakrabarti 1985; Penna et al. 2013), in section 4, I present the results from late time stages of each simulations, and, in section 5, I present the conclusions to this study.

2. NUMERICAL METHODS

We use the Athena++ code (Stone et al. 2020) that evolves the GRMHD equations of motion (**?**) on a spherical polar-like grid in Kerr-Schild coordinates. Athena++ includes speed up capabilities, such as adaptive mesh refinement (AMR), however, we do not include them in this study. Furthermore, we adopt the geometrical numerical unit convention, $G = c = 1$, and normalize the BH mass to $M = 1$, thereby normalizing the length scale to the gravitational radius $r_g = GM_{BH}/c^2$.

In this paper, we place a non-spinning BH ($a = 0$) into an equilibrium hydrodynamic torus with a Keplerian-like angular momentum profile, $l \propto r^{1/2}$, with inner edge located at $r_{in} = 10r_g$, density maximum at $r_{max} = 13.792r_g$, and outer edge at $r_{out} = 10^3 r_g$. The outer edge of the grid is located at $r = 10^4 r_g$. The torus scale height ranges from $h/r = 0.5$ at r_{max} to 1 at r_{out}. Furthermore, to allow the simulation maximum evolution times, we perform the simulations in 2D, using the $r \times \theta$.

Within the torus, we place a toroidal magnetic field with a uniform plasma $\beta = p_{gas}/p_{mag} = 5$ which eventually evolves into large-scale poloidal magnetic fields that creates a MAD. We use an effective resolution of 256×256 (where $N_r \times N_\theta$), resulting in 128 cells per disc scale height, $h/r \approx 1$.

This simulation is evolved out to $100,000r_g/c$, allowing us to observe a quasi steady state flow out to $100r_g$, which will be our primary analysis region for this paper. We analyze the mass accretion rate, bernoulli parameter and magnetic field strength for a time-averaged late-time $(80,000 - 120,000r_g/c)$ portion of the simulation, such that the accretion flow has reached steady state and the magnetic flux on the the event horizon is constant. We choose our system such that the spin of the black hole is 0, meaning that now relativistic jet will be formed (Tchekhovskoy et al. 2012). Such conditions also allow us to study an accretion flow that is unaffected by relativistic outflows.

3. DISK SOLUTIONS

In this section, I present three solutions for the initial conditions of a thick torus around a non-spinning black hole. All solutions will be presented assuming $a = 0$; for the solutions including spin, I would recommend looking at the original papers (Fishbone & Moncrief 1976; Chakrabarti 1985; Penna et al. 2013).

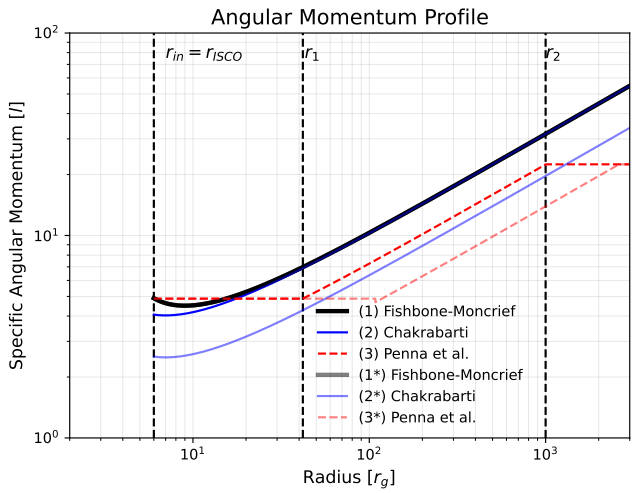

Figure 1. The specific angular momentum (l) at the midplane of our system ($\theta = \pi/2$), shown by the completely solid lines, and at the $\theta = \pi/8$ polar angle, shown by the opaque lines (starred in the legend.) The main take away, is the difference in radial behavior of the (2) and (3) profiles at different polar angles due to its dependence on the cylindrical radius, rather than spherical-polar radius.

To begin with, we define our spacetime metric as such (Carroll 2014):

$$ds^2 = -(1 - \frac{2GM}{r})dt^2 + (1 - \frac{2GM}{r})^{-1}dr^2 + r^2 d\Omega^2, \quad (1)$$

where:

$$d\Omega^2 = d\theta^2 + \sin(\theta)^2 d\phi^2. \quad (2)$$

The premise of all three solutions is to present an accretion disk that is stationary in all 4 dimensions when there are no internal forces in the accretion disk (magnetized or hydrodynamic turbulence). Therefore, when the simulations evolved, we know that their evolution and inward accretion is not a result of any initial velocity or instability we placed in the accretion disk, but instead a result of turbulences in the accretion disk created due to the magnetized and hydrodynamic forces present (Balbus & Hawley 1991; Manikantan et al. 2023 [In Prep.]).

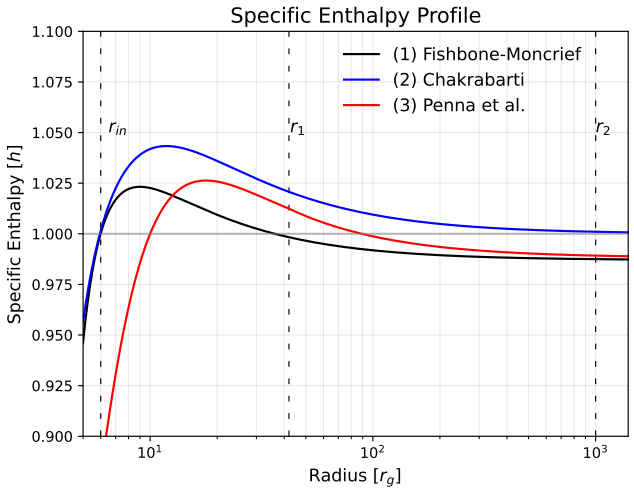

Figure 2. The specific enthalpy (h) at the midplane of our system ($\theta = \pi/2$). Enthalpy is physical when it's value is above one, otherwise, we are not inside the accretion disk and there is no value of density (or pressure or energy). We see that both the (1) FM and (2) PL solution peak early, at r $10r_g$, and the (3) Modified PL solution peaks later at about $r = 18r_g$. These peaks are common with the density peaks.

There is two key quantity to determining the properties of an accretion disk: 1. angular momentum profile, and 2. Equation(s) of State. From the angular momentum profile, we can calculate the angular velocity and enthalpy (h). Once we have the enthalpy, we can use the equations of state to solve for pressure, density and internal energy. The equation of state:

$$P = \rho\epsilon(\Gamma - 1). \tag{3}$$

We can then express each quantity in terms of the enthalpy, w:

$$\epsilon = (h - 1)/\Gamma, \tag{4}$$

then, we can express the pressure and density as:

$$\rho = [(\Gamma - 1)\epsilon/\kappa]^{1/(\Gamma-1)}, \tag{5}$$

$$P = \kappa\rho^{\Gamma}, \tag{6}$$

Where κ, the entropy, is a free parameter.

Furthermore, while the angular momentum profile of systems is usually presented as a function of the spherical radial coordinate, in the cases of the PL and Modified PL solutions, it is a function of a quasi-cylindrical radius:

$$\lambda = \sqrt{-g_{pp}/g_{tt}} \tag{7}$$

for a non-spinning BH, where g_{pp} and g_{tt} are components of the spacetime metric tensor (equation 1.)

In the case of Chakrabarti and Penna et al. solutions, the angular momentum is given by:

$$l_k(\lambda) = \sqrt{\lambda} * \mathcal{F}/\mathcal{G} \tag{8}$$

where:

$$\mathcal{F} = 1, \mathcal{G} = 1 - 2/\lambda,$$

for the non-spinning BH case. For the modified power-law torus, we introduce two radii, r_1 and r_2, that define the beginning and ending of the angular momentum's power-law behavior. Outside of those radii, the specific angular momentum is constant, as shown in figure 1.

Once we have the angular momentum for each solution, there are two distinct methods used to calculate the enthalpy of the system. The first is from the Fishbone & Moncrief solution, which provides an enthalpy profile which assumes constant angular momentum per unit inertial mass. For brevity's sake, I am not going to include the entire expression here but instead direct you equation 3.6 in the original paper. The second method, taken from Chakrabarti and cast in a simplified manner by Penna et al., uses the angular momentum profile and angular velocity to determine the enthalpy, through Euler's equation in hydrostatic equilibrium, which is then used to define pressure (P), density ρ and internal energy ϵ. The Chakrabarti and Penna solutions differ by their angular momentum profiles (fig 1).

The angular momentum profile for all three solutions have the same power-law behaviour, however, they have different magnitudes, and in the case of the Modified PL solution (3), it includes breaks at the cylindrical radius $\lambda_1 = r_1 = 42r_g$.

3.1. *Initial Enthalpy Profile*

In figure 2 we show the initial radial profile of the enthalpy at the midplane of each torus solution. Any

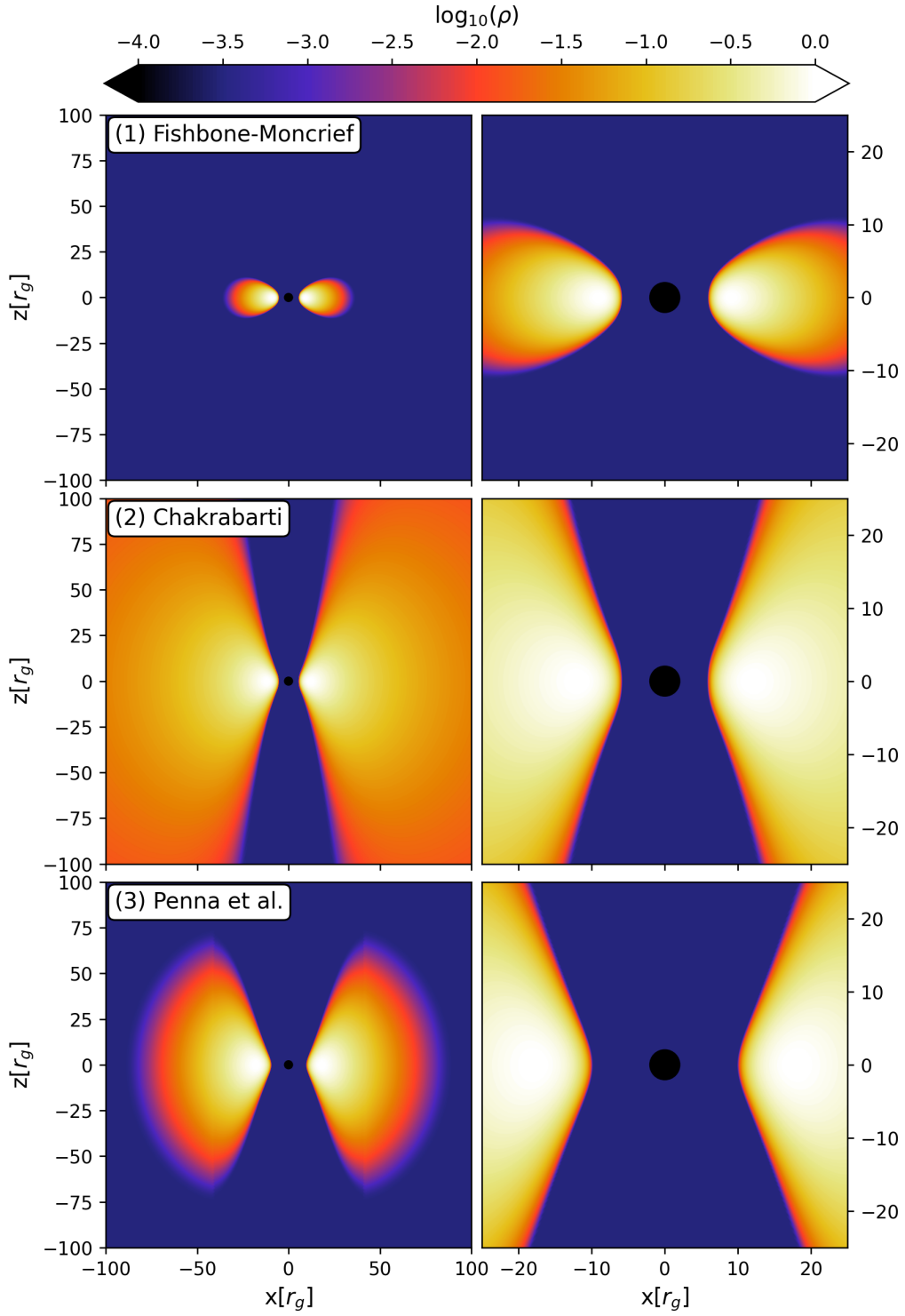

Figure 3. We present a contour plot of the gas density of the accretion disk at $t = 0$ for each of the solutions being studied. In the rows we have the (1) Fishbone-Moncrief (FM), (2) Chakrabarti (PL), and (3) Penna (Modified PL) disk solutions. We take vertical slices of the accretion disk in each case; meaning, we are looking at the $x - z$ plane. In the left column we picture the system out to $100r_g$ and in the right column out to $25r_g$.

value of enthalpy below one is not inside the initial accretion disk. Therefore, we can see the brevity of the FM torus which falls below $h = 1$ at $35r_g$; the Penna solution exists out to r $100r_g$; and, the Chakrabarti solution extends out to infinity, by choice.

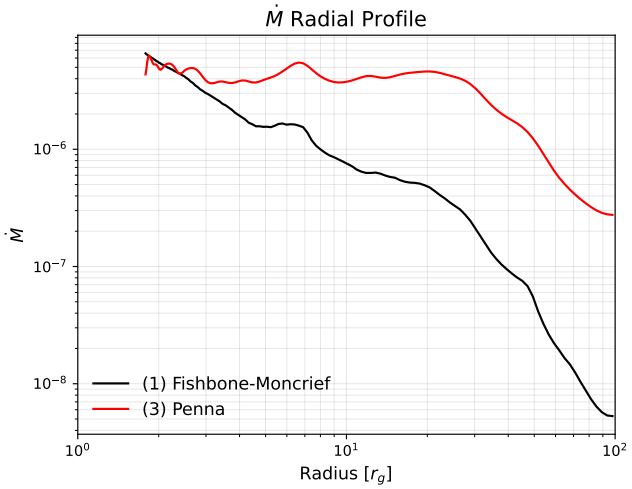

Figure 4. We show the radial dependence of the mass accretion rate for the Fishbone-Moncrief solution and the Modified PL solution. We see the viscous spreading as compared to the figure 3

. There is a strong correlation between initial conditions profile and current profile.

3.2. *Initial Density Profile*

In Figure 3, we present the initial conditions for all three systems. We take a vertical slice of the system, choosing a specific azimuthal coordinate ($\varphi = 0, \pi$) and plotting the θ and r coordinates in the $x - z$ plane.

In the top row, the FM solution, the density peaks at $r = 9r_g$ and extends out to $35r_g$. In the middle row, the PL solution, the density peaks at $r = 12r_g$ and technically extends out to $r = \infty$, but reaches about 1% ρ_{peak} at $r = 200r_g$. Finally, in the last row, the Modified PL solution, the density peaks at $18r_g$ and extends out to $90r_g$. The intial conditions for the Fishbone-Moncrief solution are taken from the existing Athena++ code, which is why it is small compared to the other two solutions.

All three disks are intialized with the same magnetic field: a single toroidal loop placed at the mid-plane of the disk and centered on the BH.

4. RESULTS

Our results show that the mass accretion rate of these systems depends heavily on the initial accretion disk set up. This, however, is not a surprise. Figure 3 shows the large discrepancy in each systems total mass within the initial conditions. The modified PL disk has a larger density at further radii, and this is reflected in the $\dot{M}$ plot as the density is driving the accretion rate up.

In figure 5, we show the later time accretion flow of the initial Fishbone-Moncrief torus. While $10,000$ r_g/c is sufficient enough to develop a meaningful accretion flow and outflows, it is not enough to reach the quasi-steady state that we would've liked. A quasi-steady state accretion flow is one that is φ and t independent. This also would mean that the accretion rate is somewhat constant with radius. Additional, longer simulations that are currently being simulated out to $100,000r_g/c$ should be able to tell us more about how the solutions differ at extreme timescales.

Lastly, at the onset of this project, I said that the bernoulli parameter would be central to understanding these systems and how they evolve. Unluckily for me, Athena++ does not have an explicitly defined Bernoulli parameter nor has it explicitly defined the variables needed to calculate it in its core outputs. Once these analysis tools ahve been developed further, we will gain an additional insight into the system.

5. CONCLUSIONS

Using the parallelized, GRMHD code Athena++ we demonstrate one aspect of the sensitivity of the system to it's initial conditions. Not only are the evolutions of the systems different, they are directly correlated to the initial conditions. However, we are seriously limited in both simulation time and resolution. Further studies need to be conducted to more carefully understand the influence of initial condition on the results of GRMHD simulations.

This is not a good, let alone groundbreaking result, but it does, at its simplest, show that our GRMHD simulations are not agnostic to initial conditions.

In the context of the class project, this research falls a little short of whats discussed in Penna et al.. The majority of the time working on this project was deciphering the physics of magnetized fluid dynamics on curved space and uncovering the unspoken assumptions and tricks (more like handwaving) that go into setting up one of these simulations. I really think that this has a lot of potential to be an interesting study and possibly even a publication!

Software: Athena++ (Stone et al. 2020)

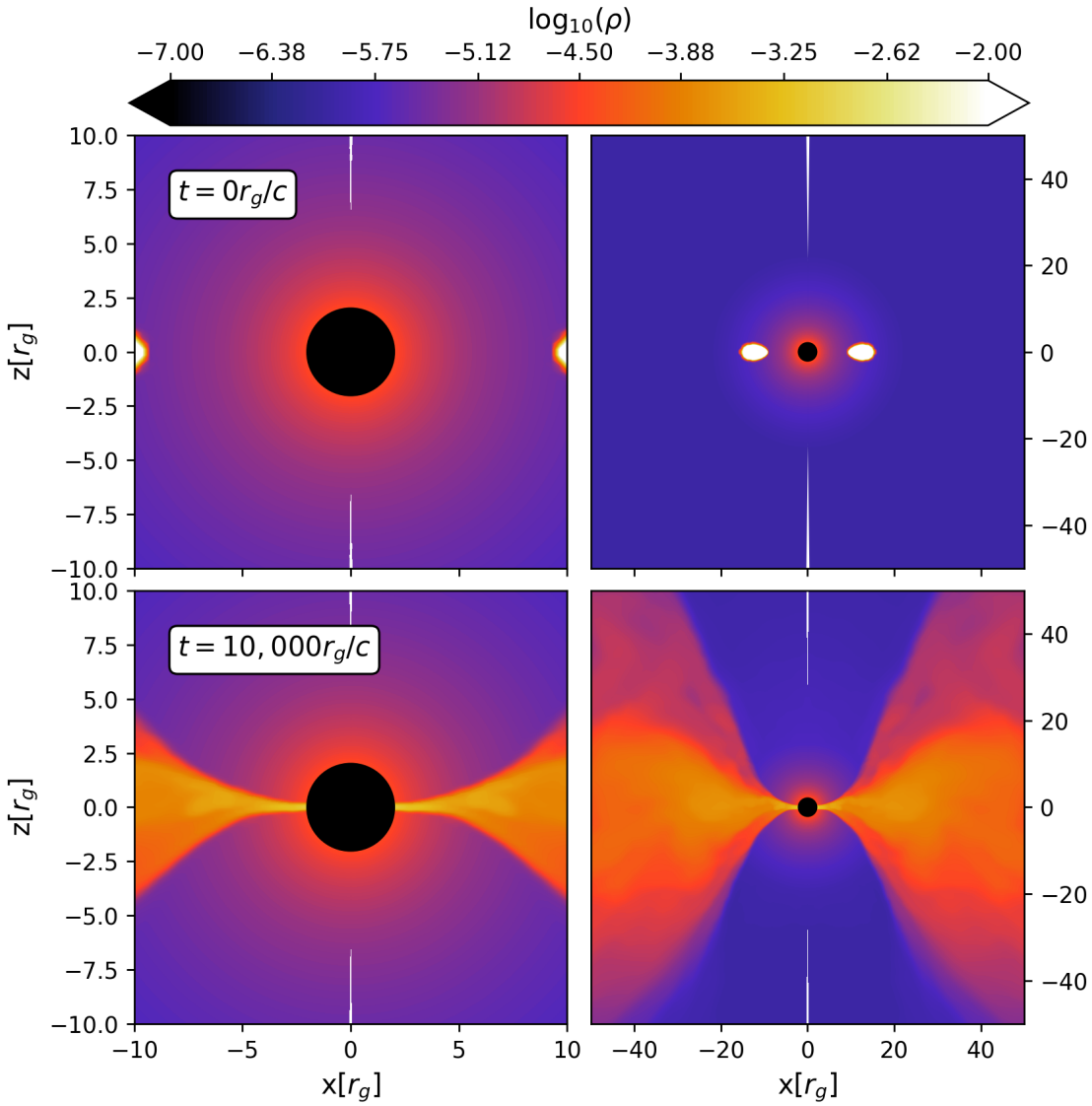

Figure 5. We present a contour plot of the gas density of the Fishbone-Moncrief simulated accretion disk at $t = 0$ and $t = 10,000 r_g/c$. We take vertical slices of the accretion disk such that we are looking at the $x - z$ plane. In the left column we picture the system out to $50 r_g$ and in the right column out to $10 r_g$. The main takeaway is the viscous spreading of the disk of the disk due to lack of external forces and advection of the matter onto the black hole. In the late time, we see the gas funneling into a narrow nozzle as it is accreted onto the BH. (Note: the white lines at the poles are a plotting artifact, not a simulation or numerical artifact.)

REFERENCES

Balbus, S. A., & Hawley, J. F. 1991, The Astrophysical Journal, 376, 214, doi: 10.1086/170270

Carroll, S. 2014 (Pearson)

Chakrabarti, S. K. 1985, The Astrophysical Journal, 288, 1, doi: 10.1086/162755

Fishbone, L. G., & Moncrief, V. 1976, The Astrophysical Journal, 207, 962, doi: 10.1086/154565

Gammie, C. F., McKinney, J. C., & Toth, G. 2003, The Astrophysical Journal, 589, 444, doi: 10.1086/374594

Liska, M. T. P., Chatterjee, K., Issa, D., et al. 2022, ApJS, 263, 26, doi: 10.3847/1538-4365/ac9966

Manikantan, V., Kaaz, N., Jacquemin-Ide, J., et al. 2023 [In Prep.]), Astrophysical Journal

Penna, R. F., Kulkarni, A., & Narayan, R. 2013, Astronomy & Astrophysics, 559, A116, doi: 10.1051/0004-6361/201219666

Stone, J. M., Tomida, K., White, C. J., & Felker, K. G. 2020, The Astrophysical Journal Supplement Series, 249, 4, doi: 10.3847/1538-4365/ab929b

Tchekhovskoy, A., McKinney, J. C., & Narayan, R. 2012, Journal of Physics: Conference Series, 372, 012040, doi: 10.1088/1742-6596/372/1/012040